

^{239}Pu alpha spectrum analysis based on PIPS detector response function and variations with vacuum and distance

Rui Shi^{1,2,3} · Xian-Guo Tuo^{1,2,3} · Huai-Liang Li³ · Jian-Bo Yang¹ · Yi Cheng¹ · Hong-Long Zheng^{2,3}

Received: 3 March 2015 / Revised: 25 September 2015 / Accepted: 15 October 2015 / Published online: 30 November 2016
© Shanghai Institute of Applied Physics, Chinese Academy of Sciences, Chinese Nuclear Society, Science Press China and Springer Science+Business Media Singapore 2016

Abstract Effect factors of the absorption of the source, air, entrance window, and dead layer of a detector must be considered in the measurement of monoenergetic alpha particles, along with statistical noise and other factors that collectively cause the alpha spectrum to exhibit a well-known low-energy tail. Therefore, the establishment of an alpha spectrum detector response function from the perspective of a signaling system must consider the various factors mentioned above. The detector response function is the convolution of an alpha-particle pulse function, two exponential functions, and a Gaussian function, followed by calculation of the parameters of the detector response function using the weighted least-squares fitting method as proposed in this paper. In our experiment, ^{239}Pu alpha spectra were measured by a high-resolution, passivated implanted planar silicon (PIPS)

detector at 10 levels of vacuum and 10 source-detector distances. The spectrum-fitting results were excellent as evaluated by reduced Chi-square (χ^2) and correlation coefficients. Finally, the variation of parameters with vacuum level and source-detector distance was studied. Results demonstrate that σ , τ_1 , and τ_2 exhibit no obvious trend of variation with vacuum in the range 2000–20,000 mTorr, and at a confidence level of 95%, the values of τ_1 and τ_2 decline in a similar fashion with source-detector distance by the power exponential function, while the value of σ declines linearly.

Keywords Alpha spectrum · Detector response function · Weighted least squares · PIPS detector

1 Introduction

The alpha spectrum measurement technique is often used in nuclear waste disposal that involves supervision and classification of transuranium nuclides such as ^{239}Pu [1], as well as in alpha aerosol radioactive monitoring [2]. In addition, qualitative and quantitative analysis of alpha nuclides by alpha spectrum measurements is a fast and economical method, although isotopic proportions can be accurately detected by a mass spectrometer.

However, almost every kind of alpha nuclides emits multiple energy of alpha rays, and the same or different nuclides commonly possess a similar energy spectrum as alpha particles. On the other hand, there are some factors that cause the alpha spectrum to exhibit a well-known low-energy tail, such as the absorption of the source, air, entrance window, dead layer, voltage bias of the detector, and the doping level of P and N regions [3]. Because of the finite resolution of a detector, spectrum unfolding is

This work was supported by the National Natural Science Foundation of China (Nos. 41374130 and 41604154), Opening Foundation of Sichuan Provincial Key Lab of Applied Nuclear Techniques in Geosciences (No. gnzds2014003), and the Open Fund of Robot Technology Used for Special Environment Key Laboratory of Sichuan Province (13zxtk04).

✉ Rui Shi
shirui0601@126.com

Xian-Guo Tuo
tuoxg@cdut.edu.cn

¹ Provincial Key Lab of Applied Nuclear Techniques in Geosciences, Chengdu University of Technology, Chengdu 610059, China

² Sichuan University of Science and Engineering, Zigong 643000, China

³ Fundamental Science on Nuclear Wastes and Environmental Safety Laboratory, Southwest University of Science and Technology, Mianyang 621010, China

necessary to accurately obtain the nuclide type and radioactive level. Thus, it is important to establish a detector response function (sometimes called a peak shape function) when analyzing overlapping alpha spectra. The detector response function depends on the parameters of peaks that can be calculated using fitting code. Moreover, these parameters are affected by the above-mentioned factors. In general, more parameters will bring better results, but will exacerbate the issues of optimization and instability [1]; therefore, the determination of parameters is critical for accurate spectrum analysis.

A number of researchers have carried out studies of these problems, and several detector response functions and fitting codes have been proposed [4–11]. For a low-background monoenergetic alpha spectrum, a detector response function that is the convolution of a Gaussian function and two exponential tailing functions has been considered the best fitting function [6–8]. Considering alpha particles emitted from a nuclide having a branching ratio, *Sánchez* [9] proposed a limited branching ratio model. Other new methods like neural networks have been applied to analyze alpha spectra [10], but the detector response function method has been regarded as the primary way to analyze alpha spectra; moreover, this method is still undergoing development [12].

In this work, the alpha spectrum detector response function was derived in detail, and in order to remove the heteroscedasticity of spectral data owing to the nonconformity of each channel’s count rate, evaluation of the parameters of the function by the weighted least-squares (WLS) method was proposed. In addition, the variations of the parameters with vacuum level and source-detector distance were studied.

2 Method

2.1 Detector response function

Figure 1 shows the process of alpha-particle emission from a nuclide to the signal generated in a multi-channel analyzer (MCA). In general, this process can be considered a signaling system. For a thin source, self-absorption can be ignored, so the emissivity of alpha particles with energy E (in keV or MeV) generated by nuclide decay can be represented by an original energy delta function $\delta(E)$ [13] [see Eq. (1)]. Alpha particles then lose energy due to the absorption of air, entrance window, and dead layer of the

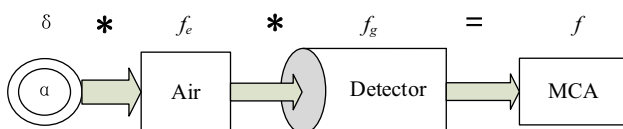


Fig. 1 Process of alpha spectrum formation

detector; in addition, incomplete charge collection results from the voltage bias and doping level of P and N regions, which is commonly assumed to be an exponential function [5, 13] [see Eq. (2)]. In the detector, electron–hole pair statistical fluctuation occurs for ionization, leading to the pulse height, which is in direct proportion to the electron–hole pairs, also exhibiting statistical fluctuation. Moreover, the electron noise of the preamplifier increases the fluctuation. These fluctuations can commonly be considered a Gaussian distribution [14] [see Eq. (3)].

We thus write

$$\delta(E - E_k) = \begin{cases} +\infty & E = E_k \\ 0 & E \neq E_k \end{cases}, \tag{1}$$

$$f_e(E) = \frac{1}{\tau} \exp\left(\frac{E}{\tau}\right), \tag{2}$$

$$f_g(E) = \frac{1}{\sigma\sqrt{2\pi}} \exp\left(\frac{-E^2}{2\sigma^2}\right), \tag{3}$$

where E_k is the mean energy of alpha particles (in keV or MeV), σ is the standard deviation of the Gaussian, and τ is the parameter of the exponential function expressed as the rate of the exponential component.

As a signaling system, alpha particles $\delta(E)$ go through two system processes of $f_e(E)$ and $f_g(E)$. Thus, the final nuclear signal from the MCA is a convolution of these three functions:

$$\begin{aligned} f(E) &= \delta(E - E_k) * f_e(E) * f_g(E) = f_e(E) * f_g(E - E_k) \\ &= \int_{-\infty}^{+\infty} f_e(E - x) f_g(x - E_k) dx \\ &= \int_{-\infty}^{+\infty} \frac{1}{\tau} \exp\left(\frac{E - x}{\tau}\right) \times \frac{1}{\sigma\sqrt{2\pi}} \exp\left(\frac{-(x - E_k)^2}{2\sigma^2}\right) dx. \end{aligned}$$

The integrals may be solved by introducing the complementary error function erfc , which is not representable with elementary functions:

$$\text{erfc}(x) = \frac{2}{\sqrt{\pi}} \int_x^{\infty} e^{-t^2} dt,$$

where

$$x = \frac{E - E_k}{\sqrt{2}\sigma} + \frac{\sigma}{\sqrt{2}\tau}.$$

The solution can be written as

$$f(E) = \frac{1}{2\tau} \exp\left(\frac{E - E_k}{\tau} + \frac{\sigma^2}{2\tau^2}\right) \text{erfc}\left[\frac{1}{\sqrt{2}} \left(\frac{E - E_k}{\sigma} + \frac{\sigma}{\tau}\right)\right].$$

$f(E)$ is the so-called detector response function (DRF), which actually is a probability density function whose

integral in the full energy region is 1, so for a certain intensity A of alpha particles, the detector response function can be described as

$$f(E) = \frac{A}{2\tau} \exp\left(\frac{E - E_k}{\tau} + \frac{\sigma^2}{2\tau^2}\right) \operatorname{erfc}\left[\frac{1}{\sqrt{2}}\left(\frac{E - E_k}{\sigma} + \frac{\sigma}{\tau}\right)\right], \tag{4}$$

where the *DRF* is determined by four parameters: mean energy E_k , Gaussian standard deviation σ , exponential parameter τ , and the area A of the peak. Figure 2 shows the *DRF* lines with $A = 1$ and different E_k , σ , and τ values. Note that the mean energy E_k mainly determines the position of the peak. The tailing of the low energy and width of the peak are determined by τ and σ , respectively. The greater the τ value, the greater the tailing, and the larger the σ value, the wider the peak.

However, n characteristic alpha rays are emitted from a nuclide with a branching ratio. Therefore, the branching ratio can be used in the *DRF* as a fixed parameter [9]. On the other hand, a single exponential function could not adequately deal with a complex alpha spectrum [6]. Thus, Eq. (4) was expanded as the following expression with two exponentials

$$f(E) = A \sum_{k=1}^n I_k \left\{ \frac{\eta}{2\tau_1} \times \exp\left(\frac{E - E_k}{\tau_1} + \frac{\sigma^2}{2\tau_1^2}\right) \times \operatorname{erfc}\left[\frac{1}{\sqrt{2}}\left(\frac{E - E_k}{\sigma} + \frac{\sigma}{\tau_1}\right)\right] + \frac{1 - \eta}{2\tau_1} \times \exp\left(\frac{E - E_k}{\tau_2} + \frac{\sigma^2}{2\tau_2^2}\right) \times \operatorname{erfc}\left[\frac{1}{\sqrt{2}}\left(\frac{E - E_k}{\sigma} + \frac{\sigma}{\tau_2}\right)\right] \right\},$$

where I_k is the branching ratio of the k th alpha energy emitted from the nuclide, which can be quoted from the

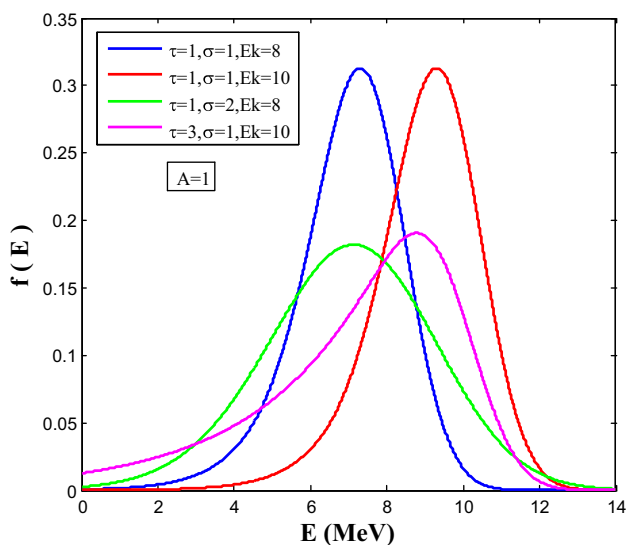


Fig. 2 (Color online) Variation of detector response function curves with parameters shown in legend

appropriate nuclear data sheet; τ_1 and τ_2 are the parameters of the exponentials; η is the proportion of the exponential; and all curves of the same nuclide are assumed to have the same parameters of σ , τ_1 , τ_2 , and η [9].

2.2 Fitting method

The substance of spectrum unfolding is obtaining the *DRF* parameters, and the normal method of obtaining them is nonlinear least-squares curve fitting [8, 9]. In order to remove the heteroscedasticity of the spectral data caused by the nonconformity of each channel's count rate, the WLS method can be applied to fit the alpha spectrum data.

The normal least-squares method used is the unweighted least-squares method (UWLS). In the radiation spectra, different values of the i th channel have different uncertainties, which makes the least-squares curve closer to the more certain points than to the less certain points. However, the variance of each channel is approximate according to the counts of each channel, and the weight of each channel is the reciprocal of the variance [15]. Thus, the WLS method used in the present work can be derived as follows, which is a matter of making the sum of weighted residual squares the minimum [16]:

$$Q = \sum_{j=1}^n \omega_j (N_j - f(x))^2 = \sum_{j=1}^n \frac{1}{N_j} (N_j - f(x))^2 = \sum_{j=1}^n \left(\frac{N_j}{\sqrt{N_j}} - \frac{f(x)}{\sqrt{N_j}} \right)^2 \rightarrow \min,$$

where ω_j is the weight, $\omega_j = 1/N_j$, $j = 1, 2, \dots, n$, N_j is the count of the j th channel, and $f(x)$ is the fitting function.

3 Experiment and results

3.1 Experimental spectrum deconvolution

The alpha spectrometer is a passivated implanted planar silicon (PIPS) detector with a 600 mm² surface area (Fig. 3). The PIPS detector has thin dead layer and therefore has high-energy resolution. The ²³⁹Pu is a thin surface source and its self-absorption can be ignored; its decay data are presented in Table 1. We considered two experimental programs to test the alpha spectrum *DRF* and study the influence of vacuum level and source-detector distance on parameters. First, 10 vacuum levels in the range 2000–20,000 mTorr in 2000-mTorr increments (1 Torr = 133.32 Pa) were used, with a 22-mm source-detector distance; second, 10 source-detector distances in the range 4–42 mm in 6-mm increments were used, at 3000 mTorr of vacuum. The testing time was 5 min, and each test was conducted five times under each condition.

Fig. 3 (Color online) Experimental alpha spectrometer with PIPS detector

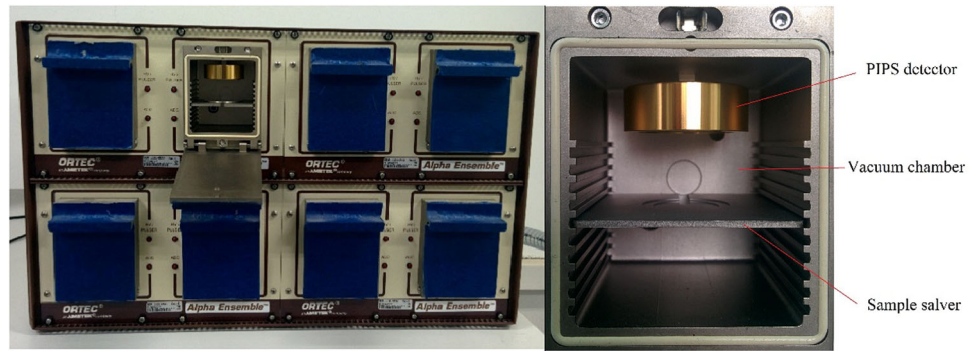


Table 1 ²³⁹Pu alpha decay data used in the present work The data are from http://www.nndc.bnl.gov/nudat2/dec_searchi.jsp

Nuclide	Energy (keV)	Intensity (%)
²³⁹ Pu	5156.6	70.77
	5144.3	17.11
	5105.5	11.94
	5076	0.078

The voltage bias of the detector was set at 50 V with a full depletion layer; the background was less than one count per hour.

The above-mentioned WLS method was then applied to fit the experimental alpha spectrum with the DRF. In the present work, reduced Chi-square (χ^2) [17–19] and the correlation coefficient (R^2) were used to evaluate the goodness of fit. The closer to 1 that χ^2 and R^2 are, the better the results:

$$\chi^2 = \frac{1}{\nu} \sum_{i=1}^r \frac{(f_i - y_i)^2}{y_i}$$

and

$$R^2 = 1 - \frac{\sum_{i=1}^r (f_i - y_i)^2}{\sum_{i=1}^r (y_i - \bar{y})^2},$$

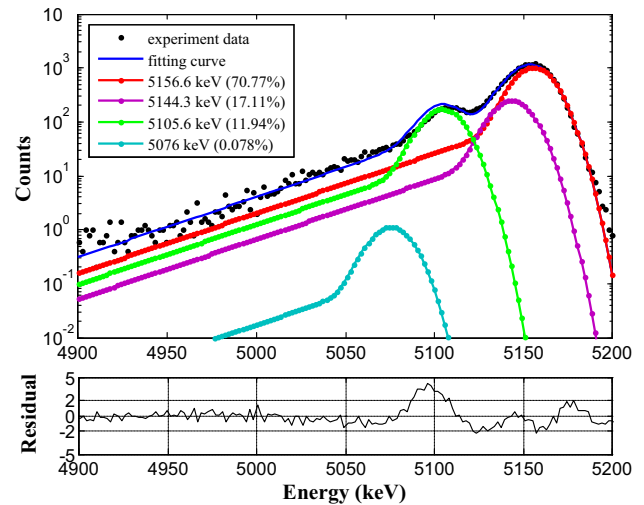


Fig. 4 (Color online) ²³⁹Pu fitting curves compared with the experimental spectrum, residual = $(f_i - y_i) / \sqrt{y_i}$

where ν is the number of degrees of freedom, $\nu = r - l - m$, l the left-hand channel of the region of interest (ROI), r the right-hand channel of the ROI, m the number of variables in the DRF, f_i the fitting data, y_i the experimental data, and \bar{y} the mean experimental data. The goodness-of-fit results for each spectrum are given in Table 2, showing that the χ^2

Table 2 Goodness of fit for ²³⁹Pu alpha spectrum unfolding using WLS and UWLS methods

Vacuum (mTorr)	WLS method		UWLS method		Distance (mm)	WLS method		UWLS method	
	χ^2	R^2	χ^2	R^2		χ^2	R^2	χ^2	R^2
2000	1.6983	0.9989	6.4154	0.9992	6	2.4517	0.9987	3.7589	0.9993
4000	1.9630	0.9985	4.6311	0.9994	10	2.0988	0.9978	4.3472	0.9984
6000	1.5995	0.9986	6.8635	0.9992	14	2.133	0.9984	10.288	0.9991
8000	1.8623	0.9986	11.051	0.9995	18	1.6224	0.9985	6.0966	0.9992
10,000	1.7861	0.9986	9.3672	0.9994	22	1.6338	0.9988	4.0188	0.9995
12,000	2.1767	0.9988	4.3005	0.9993	26	2.1496	0.9984	20.377	0.9994
14,000	1.8900	0.9987	8.3519	0.9989	30	0.9823	0.9989	4.3828	0.9992
16,000	1.8007	0.9987	8.5249	0.9995	34	1.0191	0.9989	4.6246	0.9995
18,000	2.3253	0.9983	4.3437	0.9992	38	1.0526	0.9988	2.6098	0.9994
20,000	1.4768	0.9990	6.1665	0.9996	42	0.4807	0.9994	4.3891	0.9972

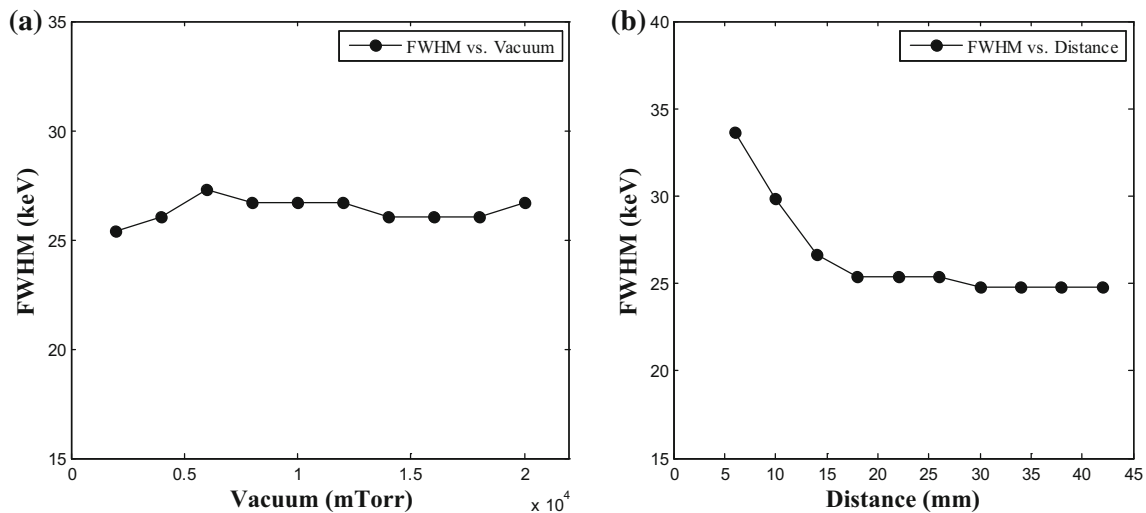


Fig. 5 FWHM variation (a) with vacuum and (b) with distance

Table 3 Parameter-fitting results under different vacuum levels with a source-detector distance of 22 mm

Vacuum (mTorr)	τ_1	σ	τ_2
2000	6.62 ± 2.40	7.95 ± 0.49	40.88 ± 6.64
4000	7.52 ± 1.63	8.65 ± 1.42	41.38 ± 7.26
6000	7.85 ± 1.65	9.03 ± 1.38	41.76 ± 7.48
8000	7.37 ± 1.81	8.93 ± 1.48	39.92 ± 7.23
10,000	7.78 ± 1.67	8.75 ± 1.40	41.91 ± 8.14
12,000	6.88 ± 2.74	8.30 ± 0.56	41.92 ± 8.30
14,000	6.99 ± 2.25	7.92 ± 0.47	41.03 ± 7.14
16,000	7.01 ± 2.40	8.14 ± 0.49	42.68 ± 7.94
18,000	7.63 ± 2.13	8.24 ± 0.60	43.43 ± 9.21
20,000	6.83 ± 2.03	8.31 ± 0.45	41.63 ± 6.70

values were 0.4807–2.4517 and the R^2 values were above 0.99. For comparison, the results obtained using the UWLS method are also given in Table 2. Apparently, the results obtained by the WLS method are better than those obtained by the UWLS method. Figure 4 shows an example of one

of the fitting curves compared with experimental data. The figure indicates that the results are excellent, but the residuals at the peak are slightly larger than other points.

3.2 Influence of vacuum and distance on parameters

Sanchez et al. [20] studied the variations of σ and τ in terms of alpha-particle curve shape with energy and concluded that “both parameters σ and τ vary as E^m with m being a number depending on the source-detector distance.” In the present work, the influence of vacuum and source-detector distance on these parameters was studied.

In the prior experiment, the full width at half maximum (*FWHM*) was calculated and its variations with vacuum and source-detector distance are described in Fig. 5. For vacuum varying between 2000 and 20,000 mTorr, the *FWHM* remains approximately constant. The vacuum results for the parameters studied obtained by fitting are given in Table 3, for a source-detector distance of 22 mm. The analysis of the data shows that σ , τ_1 , and τ_2 exhibit no obvious trend of variation with vacuum. The mean value of

Table 4 Parameter-fitting results under different source-detector distances with a vacuum level of 3000 mTorr

Source-detector distance (mm)	τ_1	σ	τ_2
6	16.32 ± 0.84	8.79 ± 1.42	86.05 ± 9.67
10	9.53 ± 0.99	9.33 ± 0.97	60.85 ± 7.09
14	8.36 ± 1.22	8.92 ± 1.12	52.22 ± 6.74
18	8.15 ± 1.20	8.53 ± 1.14	46.45 ± 6.01
22	7.99 ± 1.41	8.29 ± 1.26	40.60 ± 6.51
26	7.58 ± 2.12	8.52 ± 1.71	35.38 ± 7.38
30	7.66 ± 1.72	7.76 ± 0.47	37.66 ± 6.35
34	7.12 ± 2.52	7.42 ± 0.50	34.13 ± 6.55
38	7.23 ± 2.53	7.33 ± 0.53	34.16 ± 9.88
42	6.76 ± 2.25	7.41 ± 0.46	34.15 ± 6.43

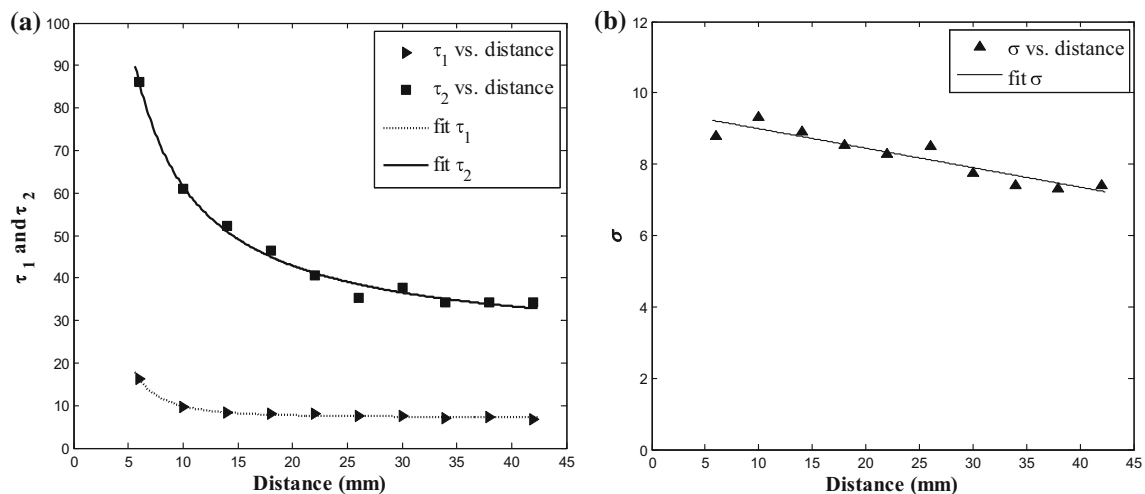


Fig. 6 Variation of fitting parameters (a) τ_1 and τ_2 and (b) σ with source-detector distance

Table 5 Fitting functions of τ_1 , τ_2 , and σ vs the source-detector distance (d) and their correlation coefficients

Fitting function	Correlation coefficient (R^2)
$\tau_1 = 723.9d^{-2.445} + 7.217$	0.9891
$\tau_2 = 355.1d^{-0.9681} + 23.37$	0.9927
$\sigma = -0.055d + 9.539$	0.8656

σ is 8.422 ± 0.7894 , that of τ_1 is 7.248 ± 0.8713 , and that of τ_2 is 41.653 ± 1.9368 . These results are in agreement with the $FWHM$ being constant. Thus, one could conclude that vacuums in the range 2000–20,000 mTorr have no impact on the alpha peak shape with a fixed source-detector distance. In other words, the absorption of air could be regarded as constant in this vacuum region.

The source-detector distance parameter-fitting results at a vacuum level of 3000 mTorr are given in Table 4, and regression curve fitting is applied to σ , τ_1 , and τ_2 versus source-detector distance in Fig. 6. Statistical analysis indicates that to a confidence level of 95%, the τ_1 and τ_2 declined in a similar fashion with the power exponential function and σ declined linearly. Table 5 lists the fitting functions of σ , τ_1 , and τ_2 . It is precisely that the parameters σ , τ_1 , and τ_2 vary with source-detector distance that results in the $FWHM$ decreasing with increasing distance, as shown in Fig. 5b; however, all three parameters do not seem to vary when the source-detector distance is larger than 22 mm.

4 Conclusion

The suitability of an alpha spectrum as a signaling system is subject to many influencing factors, so a suitable detector response function is important to unfolding the alpha

spectrum. The detector response function, which is a convolution of a pulse function, two exponential functions, and a Gaussian function, can be very suitable for the complicated and low-background alpha spectrum unfolding in ^{239}Pu . The weighted least-squares method can remove the heteroscedasticity resulting from the nonconformity of each channel's count rate, and it is excellent for alpha spectrum fitting. In addition, the WLS method can be used with gamma and X-ray radiation spectra. The initial values of the parameters, however, are very significant in the fitting process. In the present work, the variations of the DRF parameters with vacuum and source-detector distance were studied, and statistical analysis of the data showed that σ , τ_1 , and τ_2 could be regarded as constant when the vacuum was in the range 2000–20,000 mTorr. When the source-detector distance increased, τ_1 and τ_2 declined with the power exponential function and σ declined linearly. It was precisely because of the variations of these parameters that the resolution ($FWHM$) of the detector changed under different conditions, and the parameters are determined by the properties of the detector and detection conditions. There are some other factors that are not discussed in this work, such as dead layer and the doping level of P and N regions, because of the limitations of the current experimental conditions. These factors will be considered in simulations in future work.

References

1. E. García-Toraño, M.L. Aceña, G. Bortels et al., Alpha-particle emission probabilities in the decay of ^{239}Pu . Nucl. Instrum. Methods Phys. Res. A **334**, 477–484 (1993). doi:[10.1016/0168-9002\(93\)90811-U](https://doi.org/10.1016/0168-9002(93)90811-U)
2. X. Kang, D.T. Xiao, J.L. Li, Optimization of alpha energy spectrum method for measuring radon and thoron daughters in air. Nucl. Tech. **31**, 925–930 (2008). (in Chinese)

3. P.B. Rodríguez, A.M. Sánchez, F.V. Tomé, Experimental studies of self-absorption and backscattering in alpha-particle sources. *Appl. Radiat. Isot.* **48**, 1215–1220 (1997). doi:[10.1016/S0969-8043\(97\)00174-7](https://doi.org/10.1016/S0969-8043(97)00174-7)
4. R.C. Noya, E. Garcia-Torano, E. Mainegra et al., The WinALPHA code for the analysis of alpha-particle spectrum. *Nucl. Instrum. Methods Phys. Res. A* **525**, 522–528 (2004). doi:[10.1016/j.nima.2004.02.010](https://doi.org/10.1016/j.nima.2004.02.010)
5. E. Garcia-Torano, M.L. Aceña, Nolin: nonlinear analysis of complex alpha spectrum. *Nucl. Instrum. Methods Phys. Res. A* **185**, 261–269 (1981). doi:[10.1016/0029-554X\(81\)91220-9](https://doi.org/10.1016/0029-554X(81)91220-9)
6. G. Bortels, P. Collaers, Analytical function for fitting peaks in alpha-particle spectrum from Si detectors. *Appl. Radiat. Isot.* **38**, 831–837 (1987)
7. A. Martín Sánchez, F. Vera Tomé, P. Rubio Montero, Fitting of alpha spectrum application to low-level measurements. *Appl. Radiat. Isot.* **47**, 899–903 (1996)
8. A. Martín Sánchez, P.R. Montero, FITBOR a new program for the analysis of complex alpha spectrum. *Nucl. Instrum. Methods Phys. Res. A* **369**, 593–596 (1996). doi:[10.1016/S0168-9002\(96\)80058-1](https://doi.org/10.1016/S0168-9002(96)80058-1)
9. A. Martín Sánchez, P. Rubio Montero, Simplifying data fitting using branching ratios as constraints in alpha spectrometry. *Nucl. Instrum. Methods Phys. Res. A* **420**, 481–488 (1999). doi:[10.1016/S0168-9002\(98\)01179-6](https://doi.org/10.1016/S0168-9002(98)01179-6)
10. A. Baeza, J. Miranda, J. Guillén et al., A new approach to the analysis of alpha spectrum based on neural network techniques. *Nucl. Instrum. Methods Phys. Res. A* **652**, 450–453 (2011). doi:[10.1016/j.nima.2011.01.170](https://doi.org/10.1016/j.nima.2011.01.170)
11. C.J. Bland, J. Truffy, Deconvolution of alpha-particle spectrum to obtain Plutonium Isotopic Ratios. *Appl. Radiat. Isot.* **43**, 201–209 (1992)
12. S. Pommé, B. Caro Marroyo, Improved peak shape fitting in alpha spectra. *Appl. Radiat. Isot.* **2015**(96), 148–153 (2015). doi:[10.1016/j.apradiso.2014.11.023](https://doi.org/10.1016/j.apradiso.2014.11.023)
13. W. Wätzig, W. Westmeier, Alfun-A program for the evaluation of complex alpha-spectrum. *Nucl. Instrum. Methods* **153**, 517–524 (1978). doi:[10.1016/0029-554X\(78\)91001-7](https://doi.org/10.1016/0029-554X(78)91001-7)
14. E. Steinbauer, G. Bortels, P. Bauer et al., A survey of the physical processes which determine the response function of silicon detectors to alpha particles. *Nucl. Instrum. Methods Phys. Res. A* **339**, 102–108 (1994). doi:[10.1016/0168-9002\(94\)91787-6](https://doi.org/10.1016/0168-9002(94)91787-6)
15. Z.H. Wu, G.Q. Zhao, F.Q. Lu et al., *Nuclear Physics Experiment Method* (Atomic Energy Press, Beijing, 1997), pp. 1–16. (in Chinese)
16. He Xiaoqun, Liu Wenqing et al., *Applied Regression Analysis* (China Renmin University Press, Beijing, 2011), pp. 95–100. (in Chinese)
17. NIST/SEMATECH e-Handbook of Statistical Methods. <http://www.itl.nist.gov/div898/handbook/>
18. Z. Li, X.G. Tuo, R. Shi et al., Analytic fitting and simulation methods for characteristic X-ray peaks from Si-PIN detector. *Nucl. Sci. Tech.* **24**, 060206-1–060206-7 (2013)
19. Z. Li, X.G. Tuo, R. Shi et al., A statistical approach to fit Gaussian part of full-energy peaks from Si (PIN) and SDD X-ray spectrometers. *Sci. China Technol. Sc.* **57**, 19–24 (2014). doi:[10.1007/s11431-013-5427-7](https://doi.org/10.1007/s11431-013-5427-7)
20. A. Martín Sánchez, D. Caceres Marzal, Experimental study of the curve-shape variations in alpha-particle spectrometry. *Nucl. Instrum. Methods Phys. Res. A* **414**, 265–273 (1998). doi:[10.1016/S0168-9002\(98\)00663-9](https://doi.org/10.1016/S0168-9002(98)00663-9)